esa

ECOSPHERE

Carbon fluxes from a temperate rainforest site in southern South America reveal a very sensitive sink

Jorge F. Perez-Quezada,[1,2] Juan L. Celis-Diez,[3] Carla E. Brito,[1] Aurora Gaxiola,[2,4] Mariela Nuñez-Avila,[2] Francisco I. Pugnaire,[5] and Juan J. Armesto[2,4,6,]†

[1]*Departmento de Ciencias Ambientales y Recursos Naturales Renovables, Universidad de Chile, Casilla 1004, Santiago, Chile*
[2]*Instituto de Ecología y Biodiversidad, Alameda 340, Santiago, Chile*
[3]*Escuela de Agronomía, Pontificia Universidad Católica de Valparaíso, Casilla 4-D, 2260000 Quillota, Chile*
[4]*LINCGlobal, Departamento de Ecología, Pontificia Universidad Católica de Chile, Casilla 114-D, Santiago, Chile*
[5]*LINCGlobal, Estación Experimental de Zonas Áridas, Consejo Superior de Investigaciones Científicas, Ctra. de Sacramento s/n, 04120 La Cañada, Almeria, Spain*
[6]*Cary Institute of Ecosystem Studies, 2801 Sharon Turnpike, Millbrook, New York 12545 USA*

Citation: Perez-Quezada, J. F., J. L. Celis-Diez, C. E. Brito, A. Gaxiola, M. Nuñez-Avila, F. I. Pugnaire, and J. J. Armesto. 2018. Carbon fluxes from a temperate rainforest site in southern South America reveal a very sensitive sink. Ecosphere 9(4):e02193. 10.1002/ecs2.2193

Abstract. Ecosystems where carbon fluxes are being monitored on a global scale are strongly biased toward temperate Northern Hemisphere latitudes. However, forest and moorland ecosystems in the Southern Hemisphere may contribute significantly to the global and regional C balance and are affected by different climate systems. Here, we present the first data from an old-growth forest representative of temperate, broad-leaved rainforests from southern South America. Carbon fluxes monitored over two years using the eddy covariance technique showed that this rainforest acts as an annual sink (-238 ± 31 g C/m^2). However, there were significant pulses of carbon emission associated with dry episodes during the summer months (i.e., peak of the growing season) and periods of significant carbon fixation during the cold austral winter, indicating that the carbon balance in this forest is very sensitive to climate fluctuations. The carbon fixation surges in winter seem to be related to the mild temperatures recorded during this period of the year under the prevailing oceanic climate. Winter carbon gain was more relevant in determining the annual carbon balance than summer pulse emissions. Regarding the annual carbon balance, this southern forest resembles the patterns observed in montane tropical forests more than the behavior of narrow-leaved evergreen temperate forests from the Northern Hemisphere. These patterns make this southern forest type relevant to understanding the mechanisms and thresholds that control ecosystem shifts from carbon sinks and sources and will provide key data to improve global dynamic vegetation models.

Key words: AMERIFLUX; Chile; Chiloé Island; eddy flux; evergreen; FLUXNET; North Patagonian rainforest; Southern Hemisphere.

Received 28 January 2018; accepted 5 February 2018; final version received 13 March 2018. Corresponding Editor: Debra P. C. Peters.

†**E-mail:** jarmesto@bio.puc.cl

Introduction

Understanding carbon fluxes from forests and other terrestrial ecosystems worldwide is critical for predicting long-term trends in carbon dynamics and balance in the face of increasing anthropogenic carbon emissions and recent climate change (Friend et al. 2007). Carbon fluxes are now being monitored widely from terrestrial ecosystems worldwide using

the eddy covariance method (Baldocchi 2014). Despite the fact that there is a geographically broad database of carbon flux monitoring, we are still far from having a complete picture of carbon exchanges for all ecosystem types. Most sites where data are being collected are restricted to temperate and boreal latitudes, with a small sample of tropical woodlands and grasslands (Luyssaert et al. 2007, Baldocchi 2008). A review by Luyssaert et al. (2007) showed that from 513 forest sites with data on carbon fluxes at the ecosystem level, only 21 were located in the Southern Hemisphere. Consequently, in the context of biogeochemical cycles, there is a critical gap of information regarding terrestrial ecosystems at temperate and sub-Antarctic latitudes in the Southern Hemisphere (Luyssaert et al. 2007, 2008). This gap is particularly relevant in the case of southern South American (SSA) forests, which represent the largest expanse of continuous continental forests at high latitudes in the Southern Hemisphere and the closest forested area to Antarctica, subjected to still poorly understood climatic systems, dominated by westerly wind flows and the Antarctic polar oscillation. In this paper, we provide the first data on ecosystem-level carbon exchanges from a temperate forest site in SSA, which serves to characterize the behavior of a broad-leaved, evergreen, old-growth forest and contributes to fill a gap in the information about carbon fluxes from forest ecosystems at austral high latitudes.

Evergreen temperate rainforests and sub-Antarctic forests, extending over 20 degrees of latitude along the southwestern rim of South America, have only recently been incorporated into the global monitoring of ecosystem dynamics (Armesto et al. 2009, Rozzi et al. 2012). These forests have attracted particular interest because they are located in an area of the planet where storms originate directly over the southern Pacific Ocean, hence receiving rainfall largely free of industrial contaminants (Hedin et al. 1995, Weathers et al. 2000). In contrast to their Northern Hemisphere counterparts, high-latitude forests of SSA remain one of the last wilderness refuges in the planet where the human population density is low and anthropogenic transformations of the wild landscape are still contained (Mittermeier et al. 2003).

Long-term assessment of carbon fluxes in high-latitude rainforests in SSA can be a unique source of information on future trends in net carbon exchange in a region currently facing warming and declining rainfall, which could severely depress forest growth in the coming decades (Gutiérrez et al. 2014). Since industrial pollution and atmospheric contaminants in this part of the world are likely to remain low compared to other temperate regions in the planet, monitoring carbon exchange from broad-leaved southern temperate forests opens up new opportunities for comparative studies of responses to climate change across biomes and sites with contrasting histories of industrial impact. More importantly, long-term monitoring can add site-based data from high-latitude Southern Hemisphere forests to improve dynamic global vegetation models.

Here, we analyze the first two years of carbon flux data from a new long-term study site in an old-growth, broad-leaved, evergreen forest of SSA. To our knowledge, this is the first record of ecosystem carbon exchanges from SSA and one of the three currently active sites in temperate regions of the Southern Hemisphere (FLUXNET 2016). The study was aimed at exploring the following questions, intended to anticipate long-term trends: (1) Do the SSA old-growth rainforests act as a carbon sink or source? (2) What are the main environmental drivers of the different carbon flux components in this ecosystem? (3) How can the carbon balance of this forest be characterized in relation to other forests of the world?

Materials and Methods

Site description and climate setting

Our field site has been classified as an old-growth stand of the North Patagonian forest type (Aravena et al. 2002), with a mixed canopy (25 m tall) dominated by *Nothofagus nitida* (Nothofagaceae), *Drimys winteri* (Winteraceae), and the broad-leaved conifers *Podocarpus nubigenus* and *Saxegothaea conspicua* (both Podocarpaceae; Table 1). Podocarps can reach 400 yr of age with a trunk diameter at breast height of 115 cm (Gutiérrez et al. 2004). This forest has a dense subcanopy layer (up to 10 m in height) of *Tepualia stipularis* (Myrtaceae), *Crinodendron hookerianum* (Elaeocarpaceae), and *Caldcluvia paniculata*

Table 1. Tree species recorded within a 1-ha permanent plot of North Patagonian old-growth temperate rainforest at Senda Darwin Biological Station, Chile (42° S).

Tree species	Family	Density (ind./ha)	Basal area (m^2/ha)	dbh† mean ± SE (cm)	dbh min–max (cm)
Amomyrtus luma	Myrtaceae	52	0.29	7.01 ± 0.65	4–30
Amomyrtus meli	Myrtaceae	10	0.09	9.26 ± 1.73	5–21
Crinodendron hookerianum	Elaeocarpaceae	250	0.96	6.6 ± 0.15	4–22
Caldcluvia paniculata	Cunoniaceae	321	2.33	7.6 ± 0.33	4–80
Drimys winteri	Winteraceae	205	3.15	11.25 ± 0.58	4–54
Gevuina avellana	Proteaceae	43	0.15	6.26 ± 0.27	4–12
Laureliopsis philippiana	Monimiaceae	3	0.065	13.23 ± 7.16	5–27
Myrceugenia parvifolia	Myrtaceae	13	0.038	6.06 ± 0.32	4–8
Nothofagus nitida	Nothofagaceae	130	13.19	29.05 ± 1.86	4–112
Podocarpus nubigenus	Podocarpaceae	189	9.31	19.22 ± 1.17	4–111
Raukaua laetevirens	Araliaceae	8	0.34	18.45 ± 5.30	4–45
Saxegothaea conspicua	Podocarpaceae	140	3.37	12.53 ± 1.04	4–80
Tepualia stipularis	Myrtaceae	1992	26.67	10.70 ± 0.17	4–103
Weinmannia trichosperma	Cunoniaceae	14	0.99	19.04 ± 6.41	4–94

Note: †dbh, diameter at breast height; SE, standard error.

(Cunoniaceae). Many vines and epiphytes, both vascular plants and ferns, cover the tree trunks (Muñoz et al. 2003). The understory is occupied by dense patches of native bamboo (*Chusquea valdiviensis*), tree seedlings and saplings, and a continuous carpet of cryptogams (mosses, lichens, and liverworts).

An eddy covariance system to measure carbon exchange between the forest and the atmosphere was set up over an area of approximately 100 ha, in a rural landscape mosaic of pastures and forest patches, 15 km east of Ancud, on northern Chiloé Island (41°52′ S, 73°40′ W; Fig. 1A), in the Senda Darwin Biological Field Station (SDBS), a private protected research area (Carmona et al. 2010). The site is currently linked to the networks AMERIFLUX and FLUXNET (code CL-SDF) and to the International Long-Term Ecological Research network (ILTER).

Soils over the entire landscape originated from Pleistocene moraine fields and glacial outwash plains (Aravena et al. 2002). Forest soils are wet and organic, with a saturated gley layer locally frequent at 30–60 cm depth (Hedin et al. 1995) and high fine root biomass in the first 15 cm. The prevailing climate is wet temperate with a strong oceanic influence (Di Castri and Hajek 1976). Meteorological records at SDBS (1999–2016) indicate a mean annual temperature of 9.7°C, with a monthly maximum of 14.1°C usually in January (austral summer) and a monthly minimum of 5.8°C usually in July (austral winter). Annual precipitation for the period 1999–2016 ranged between 1326 mm and 2714 mm (2016 and 2002, respectively), with an average of 2087 mm. Global circulation models predict that by the year 2100 in the Chilean Lake District (39–40° S), mean annual temperatures could increase by approximately 1.5°C and precipitation could decline by 10–20%, with decreases concentrated in the spring–summer periods (October–March; IPCC 2013).

Study design and instrumentation

The eddy-flux tower was set in an old-growth stand of North Patagonian rainforest. The prevailing, stronger winds come from the northwest (Fig. 1B), and therefore, the tower and instrumentation were located near the edge of the forest stand facing the opposite direction (Fig. 1C). In this way, we maximized the fetch, which is the distance from the tower to the border of the ecosystem being monitored, in the prevailing wind direction. To install the equipment above the canopy, we followed the manufacturer's recommendation of adding 10 m to the zero-displacement height with respect to the top of the canopy (estimated as 2/3 of the canopy height); hence, the sensors were located at the top of a 42-m tower (Fig. 1D).

To estimate the balance of carbon fluxes or net ecosystem exchange (NEE), we used a closed-path

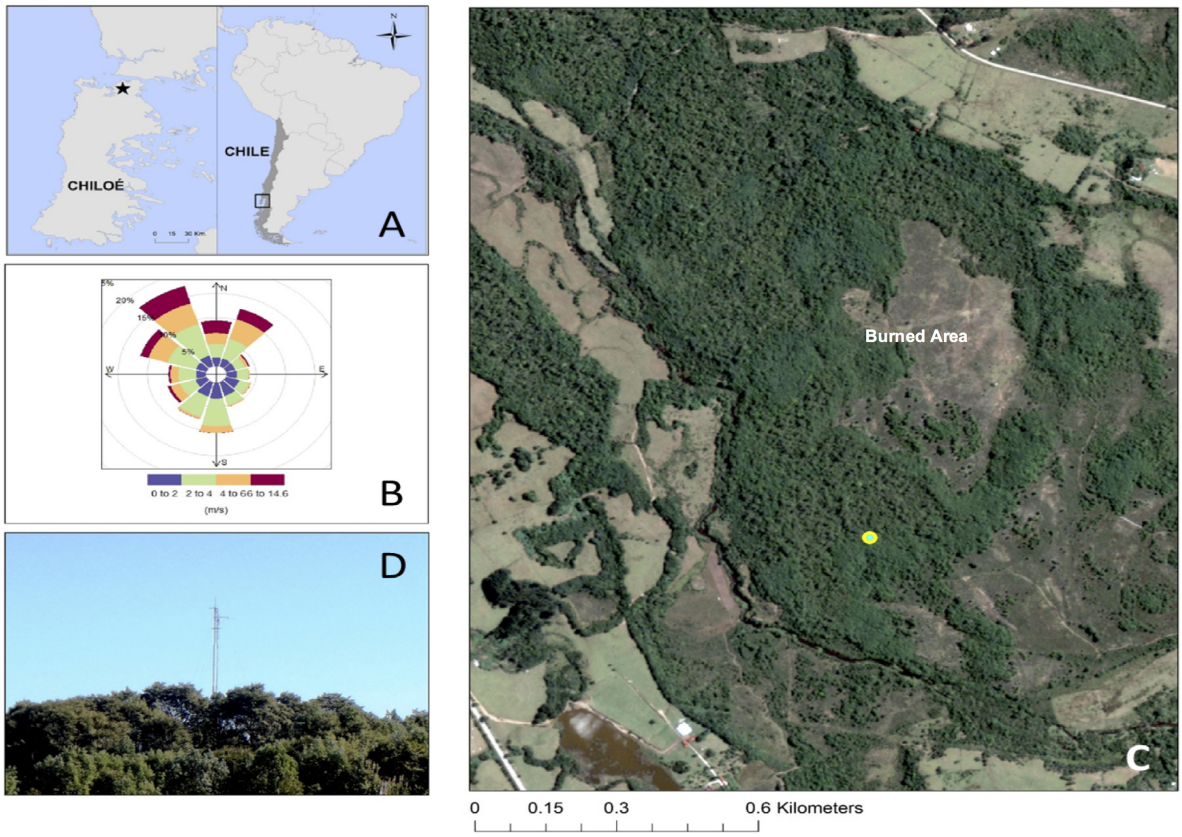

Fig. 1. (A) Location of Senda Darwin Biological Station on northern Chiloé Island; (B) wind rose of data collected during two years at the top of the 42-m tower; (C) location of the tower with the eddy covariance instrumentation (yellow dot; photograph: Google Earth), within a 100-ha forest patch on the rural landscape. Brown areas above and below the forest fragment correspond to successional, post-fire shrublands burned 50 yr ago and earlier; (D) view of the eddy-flux tower, emerging 18 m above the forest canopy (photograph: Jorge Perez-Quezada).

eddy covariance system (CPEC200; Campbell Scientific, Logan, Utah, USA) set on top of the tower (Fig. 1D). Carbon dioxide (CO_2) NEE was estimated at a 10 Hz frequency (i.e., 10 times per second) using an infrared gas analyzer (IRGA, model EC155; Campbell Scientific, Logan, Utah, USA), combined with a three-dimensional sonic anemometer (model CSAT3A; CSI), which determines the vertical component of wind speed, installed next to the IRGA. Eddy covariance carbon flux measurements were averaged every 30 min and recorded by a data logger (model CR3000; CSI). Additionally, the system recorded the following micrometeorological variables: photosynthetically active radiation (PAR, model LI-190; LI-COR, Lincoln, Nebraska, USA), total precipitation (model 52202; RM Young, Traverse City, Michigan, USA), and air temperature (model HMP155; Vaisala, Helsinki, Finland). Soil temperature and volumetric water contents were measured at 5 cm depth at three locations within 15 m of the tower using temperature probes (model TCAV; CSI) and water content reflectometers (model CS616; CSI).

Carbon flux data quality control

Quality control and corrections for ecosystem carbon exchange were necessary due to several issues that included, among others, the lack of turbulence. Corrections were performed over the raw binary data using the EddyPro software (version 4.2.1; LI-COR). Quality checks were done by a micrometeorological test (i.e., steady-state test) and the developed turbulent conditions test

(Mauder and Foken 2004). The footprint of carbon flux, that is, the area from which the carbon exchange is being assessed, was calculated according to Kljun et al. (2004). We discarded data when the footprint exceeded the fetch, which varied depending on the wind direction (Fig. 1C). The results of quality control and correction processes were analyzed using the EddyPro output of quality level, which assigns 0 to the best and 2 to the worst estimated flux values, keeping in this case data of qualities 0 and 1. After this analysis, 26% of the field data were kept and used for further analyses. Data excluded were more than the typical range for this type of carbon flux measurements (20–60%; Moffat et al. 2007) due to a two-month failure of the system (30 April–1 July 2015), which required factory recalibration.

A gap-filling process was performed to fill in missing data, considering NEE as the combination of carbon flux and storage term. Gap-filling data were obtained using the REddyProc R package developed by the Max-Planck Institute for Biogeochemistry. This package considers the covariation of ecosystem-level carbon fluxes with micrometeorological variables (measured simultaneously) and the temporal autocorrelation of carbon fluxes (Reichstein et al. 2005). As a result, NEE is partitioned into gross primary productivity (GPP) and ecosystem respiration (R_{eco}), using the relationship of NEE with temperature at night (Reichstein et al. 2005) or with light during daytime (Lasslop et al. 2010). For the two-month period when the system failed, we used a different gap-filling process, that is, a multivariate linear model considering the following variables: volumetric soil water content, air temperature, and PAR ($R^2 = 0.75$).

During the period when we measured carbon fluxes using eddy covariance, we also monitored soil respiration (R_s) every hour using an Automated Soil Flux System (LI-8100; LI-COR) connected to a multiplexer (model LI-8150; LI-COR) and three closed chambers used for long-term measurement (model LI-8100-104; LI-COR). Soil respiration was not partitioned in heterotrophic and autotrophic components, and therefore, the term R_s integrates both root and microbial respiration. Here, we show the first two years of measurements, starting in September 2013.

Modeling carbon fluxes

To analyze the effect of environmental drivers on ecosystem carbon fluxes (GPP, R_{eco}, and R_s) and their seasonal and annual variability, we fitted a set of non-linear models to the daily flux data. For modeling the effect of light on GPP, we used the light-response model proposed by Falge et al. (2001):

$$\mathrm{GPP} = \frac{\alpha \cdot \mathrm{PAR} \cdot \mathrm{GPP_{OPT}}}{\sqrt{(\mathrm{GPP_{OPT}})^2 + (\alpha \cdot \mathrm{PAR})^2}}$$

where α is the initial slope of the rectangular hyperbolic curve or the ecosystem quantum yield (g CO_2/mol quantum); and GPP_{opt} is the GPP (g $CO_2 \cdot m^{-2} \cdot d^{-1}$) at optimum PAR (mol quantum $\cdot m^{-2} \cdot d^{-1}$).

For modeling R_{eco} and R_s, we used the exponential equation proposed by Reichstein et al. (2005):

$$R = R_{10} \cdot e^{\lfloor E_0 \cdot (1/(T_{ref} - T_0) - 1/(T - T_0)) \rfloor}$$

where R_{10} is the respiration at 10°C (g $CO_2 \cdot m^{-2} \cdot d^{-1}$); E_0 is the temperature (K) analogous to activation energy; T_{ref} is the reference temperature = 283.15 K (10°C); T_0 is a constant at 227.13 K (−46.02°C); and T is the temperature (K) of either air or soil.

For fitting the models, we used the curve fitting toolbox of Matlab R2015a (The MathWorks, Natick, Massachusetts, USA), based on Coleman and Li (1994). To detect outliers, we used the concept of median absolute deviation (MAD; Leys et al. 2013), which involves finding the median of the absolute deviations from the median of the residuals:

$$\mathrm{MAD} = bM(|R_i - M(R_i)|)$$

where R_i is the series of residuals from a statistical model, M is the median of the series, and b is a constant (1.4826) used when normality of data is assumed. An observation was defined as an outlier when its residual fell outside the ±3 MAD range. After outliers were excluded, the models were fitted again.

Results

Seasonal trends and annual balance of carbon fluxes

Net ecosystem exchange was predominantly negative during the austral spring and summer

periods (October–March) in both years of study (Fig. 2A). Overall, total carbon emissions (R_{eco}) and uptake (GPP) were similar during the first two years of measurement, making the net ecosystem balance (NEE) regularly close to neutral: some periods of carbon emissions (during the growing season), followed by others of carbon uptake (during the low-plant-activity period).

The maximum values of GPP, R_{eco}, and R_s reflect the climatic seasonality of the system (Fig. 2A), where maximum biological activity (Fig. 2A) was strongly coupled with daily temperatures and PAR levels (Fig. 2B). Although precipitation is lower in summer and soil water content is relatively lower, overall levels of soil water content remained high inside the forest (Fig. 2C). In the years studied, wet and cool winters were characterized by reduced biological activity, causing R_s to account for nearly 100% of R_{eco} during the winter but to represent only 50% of R_{eco} during the summer (Fig. 2A).

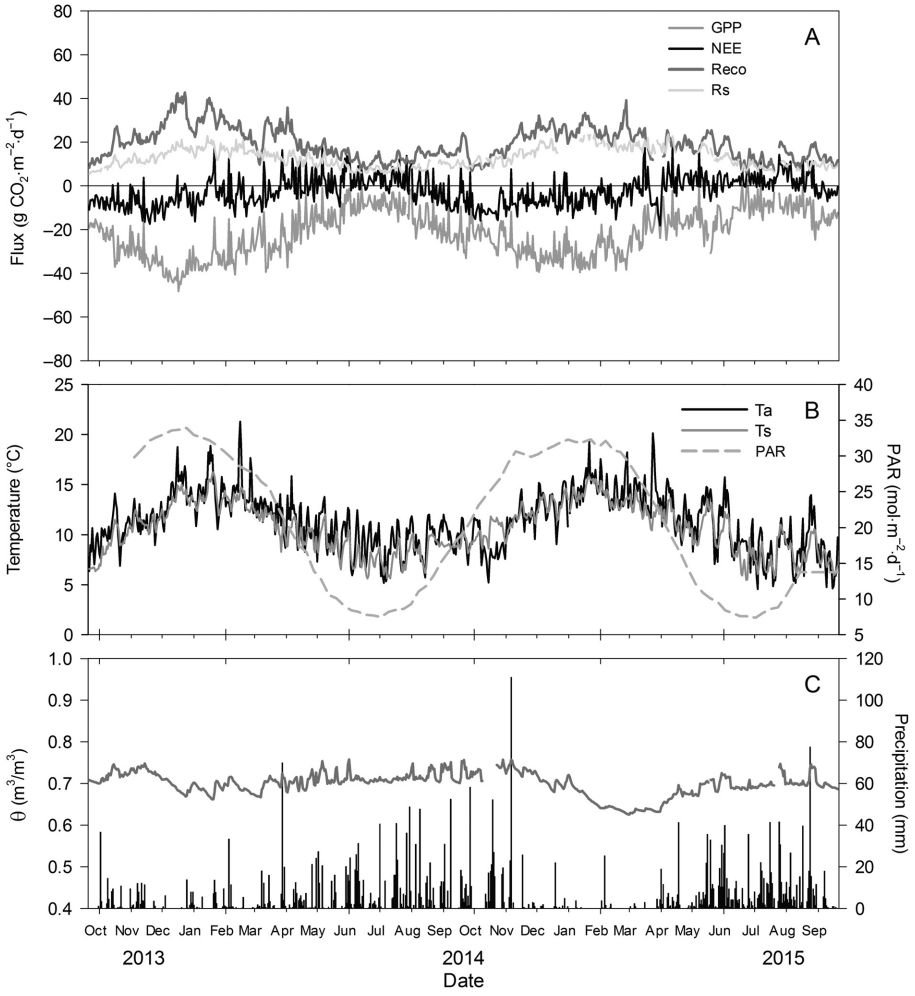

Fig. 2. Carbon fluxes and environmental variables, from September 2013 to September 2015, for an old-growth temperate rainforest of southern South America. Data are daily values of (A) gross primary production (GPP), net ecosystem exchange (NEE), ecosystem respiration (R_{eco}), and soil respiration (R_s); (B) air temperature (T_a), soil temperature at 5 cm depth (T_s), and photosynthetically active radiation (PAR); and (C) volumetric soil water content (θ; line) and precipitation (bars). In panel A, negative values imply a downward flux or carbon uptake from the ecosystem, while positive values are emissions. Values of GPP and R_{eco} are the result of nighttime partitioning; values of daytime partitioning are presented in Appendix S1.

Table 2. Carbon fluxes (g C·m^{-2}·period^{-1}) and micrometeorological variables by season and by year in an old-growth, North Patagonian temperate rainforest.

	2013–2014					2014–2015				
Variable	Spring	Summer	Fall	Winter	Year	Spring	Summer	Fall	Winter	Year
Fluxes†										
GPP	−753	−770	−390	−356	−2270	−669	−706	−396	−270	−2041
R_{eco}	554	674	437	341	2005	471	612	416	317	1815
NEE	−200	−96	47	−11	−260	−199	−95	24	53	−216
R_s	294	400	261	215	1169	337	464	379	226	1405
Micromet.‡										
P	207	258	916	831	2211	412	128	686	999	2225
T_a	11.1	14.4	10.9	9.8	11.5	10.9	14.4	12.0	8.4	11.4

Note: NEE, net ecosystem exchange; GPP, gross primary productivity; R_{eco}, ecosystem respiration; R_s, soil respiration; P (mm), mean precipitation; T_a (°C), air temperature, for the study period.

† Negative fluxes indicate ecosystem carbon uptake.

‡ Mean (mm) P per season: spring, 370.4; summer, 285.1; fall, 642.99; and winter, 713.3. Mean T_a per season: spring, 10.63; summer, 12.9; fall, 8.8; and winter, 7.4. These mean values represent the 1999–2016 period.

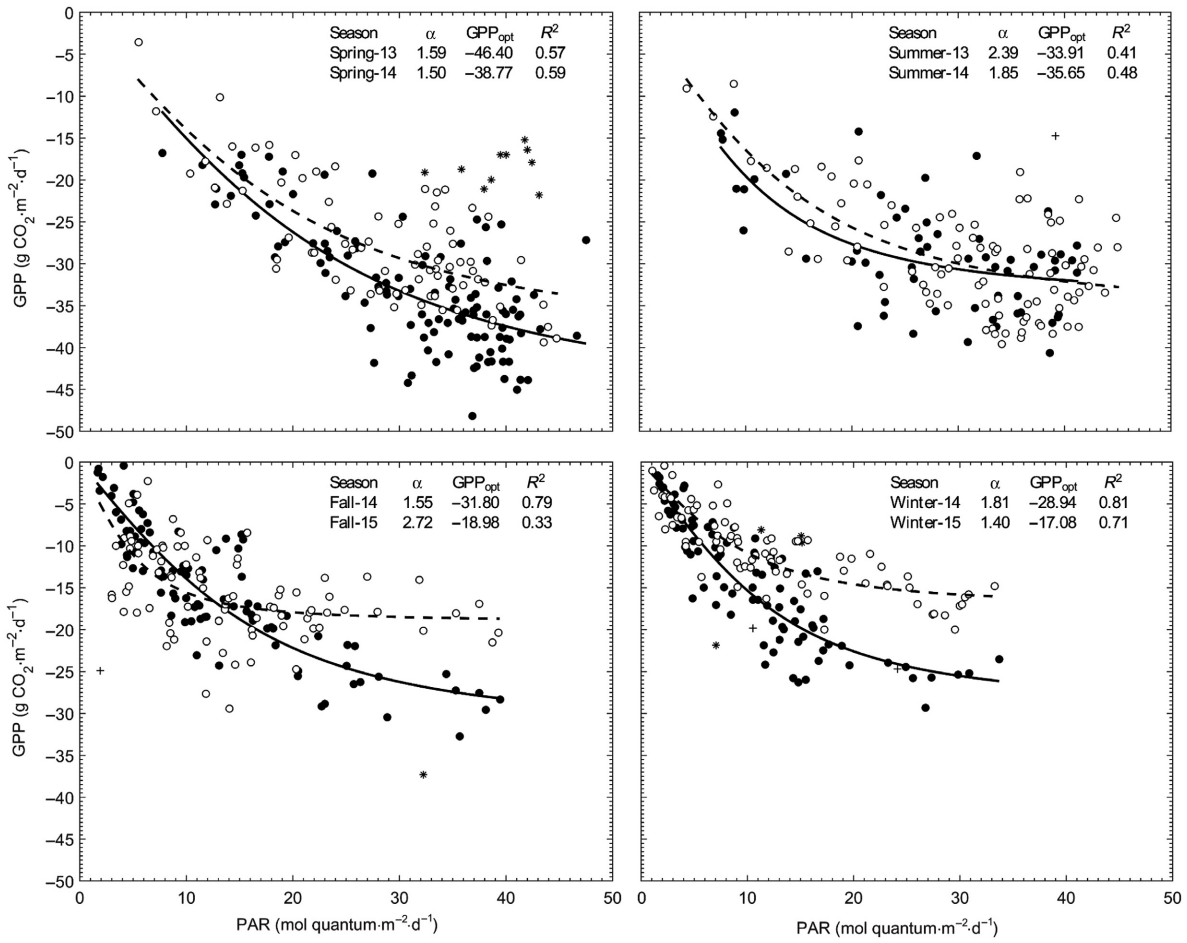

Fig. 3. Daily relation of gross primary productivity (GPP) and photosynthetically active radiation (PAR) in the four seasons for each of the two years of the study. Solid circles and lines represent the first-year (2013–2014) data and non-linear models, respectively, while open circles and dashed lines represent the second year (2014–2015). Asterisks represent observations defined as outliers for the first-year data, while crosses represent the same for the second year.

Nevertheless, pulses of significant carbon assimilation did occur during the cool periods, likely due to the moderate temperatures common to the oceanic climate setting (Fig. 2B).

Seasonal data (Table 2) show that average GPP of spring and summer (−724.7 g C/m^2) more than doubled that of fall and winter (−352.8 g C/m^2) during the two years of measurements. Both R_{eco} and R_s responded positively to increases in air and soil temperatures during summer. Despite high R_{eco} values, the ecosystem still showed an overall tendency to fix more carbon during the summer. Approximately 80% of the precipitation in this evergreen forest falls during the fall–winter period, which is also the coldest period, and according to our data, this is when the ecosystem can become a net carbon source (Table 2).

If we look at the two years independently, more carbon was captured (NEE = −260 g C/m^2) during the first year than in the second year (NEE = −216 g C/m^2), which depends primarily on fluxes during fall–winter (Table 2). In fact, records for winter 2014 showed that the forest was a carbon sink (Table 2).

Drivers of change in carbon fluxes

Non-linear models represented well the relation between PAR and GPP for all seasons and years (Fig. 3). As expected, the maximum

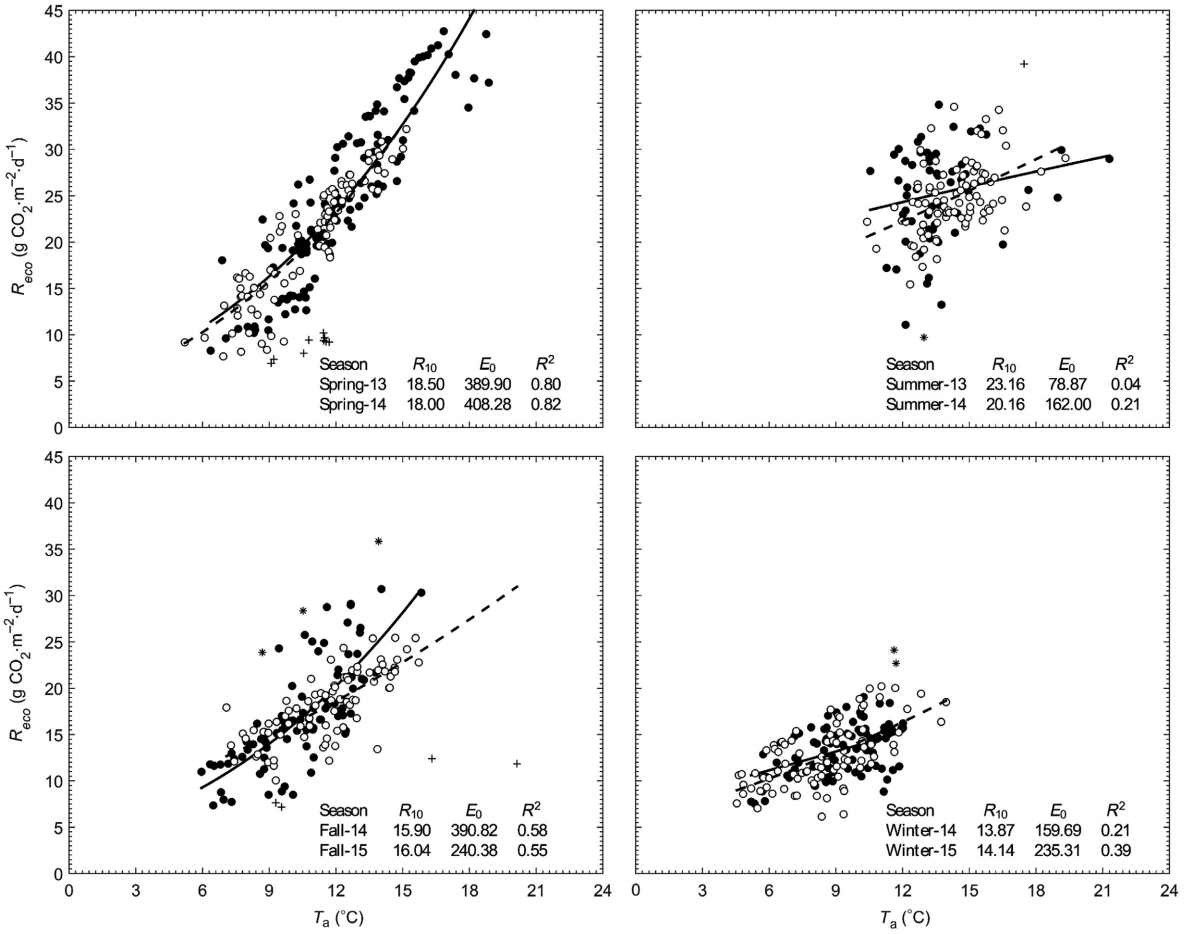

Fig. 4. Relation between daily ecosystem respiration and air temperature in the four seasons for the two years of the study. Solid circles and lines represent the first-year (2013–2014) data and non-linear models, respectively, while open circles and dashed lines represent the second year (2014–2015). Asterisks represent observations defined as outliers for the first-year data, while crosses represent the same for the second year.

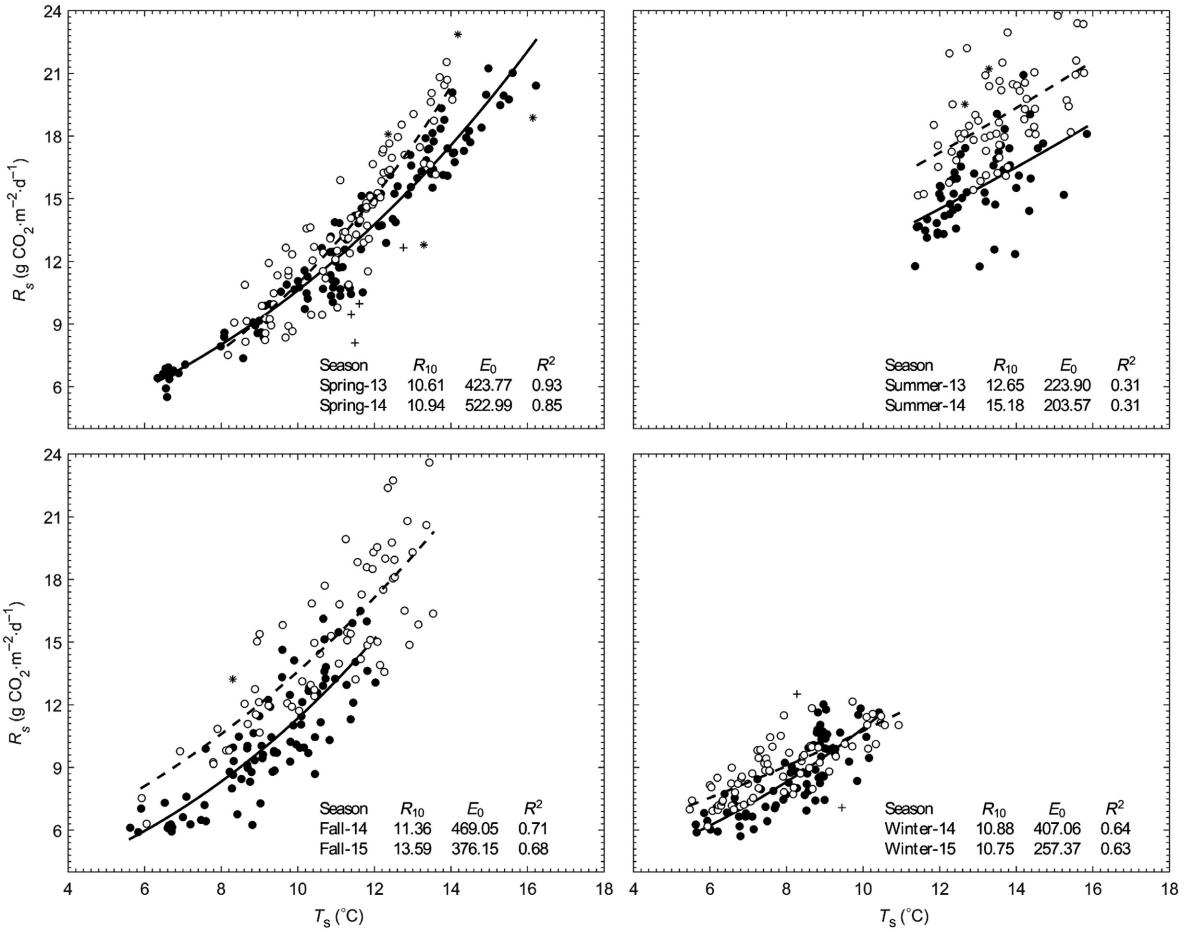

Fig. 5. Relation between daily soil respiration and soil temperature in the four seasons for the two years of the study. Solid circles and lines represent the first-year (2013–2014) data and non-linear models, respectively, while open circles and dashed lines represent the second year (2014–2015). Asterisks represent observations defined as outliers for the first-year data, while crosses represent the same for the second year.

levels of C fixation (GPP_{opt}) were observed during spring (approximately −40 g $CO_2 \cdot m^{-2} \cdot d^{-1}$), followed by summer, fall, and winter. The first study year (2013–2014) showed higher maximum C fixation compared to the second year for all seasons except summer (Fig. 3).

Ecosystem respiration was dependent on air temperature (T_a), which was well represented by a non-linear model for all seasons except summer (Fig. 4). Ecosystem respiration at 10°C (R_{10}) was higher during summer (~21.5 g $CO_2 \cdot m^{-2} \cdot d^{-1}$), followed by spring, fall, and winter. In the case of R_{eco}, model parameters did not differ much between years (Fig. 4).

The same type of non-linear model was used to represent the relationship between R_s and soil temperature (T_s; Fig. 5). Summer R_{10} values were also the highest (~14 g $CO_2 \cdot m^{-2} \cdot d^{-1}$), but in this case, they were followed by fall values, while spring and winter showed similar lower values. Soil respiration was higher during the second year for similar levels of T_s (Fig. 5).

To analyze the potential impacts on carbon balance of dry summers, which are expected to increase in frequency under climate change in the coming decades, we focused on measurements taken during both summer periods included in this study (2013–2014 and 2014–2015). Our records showed a mean summer air

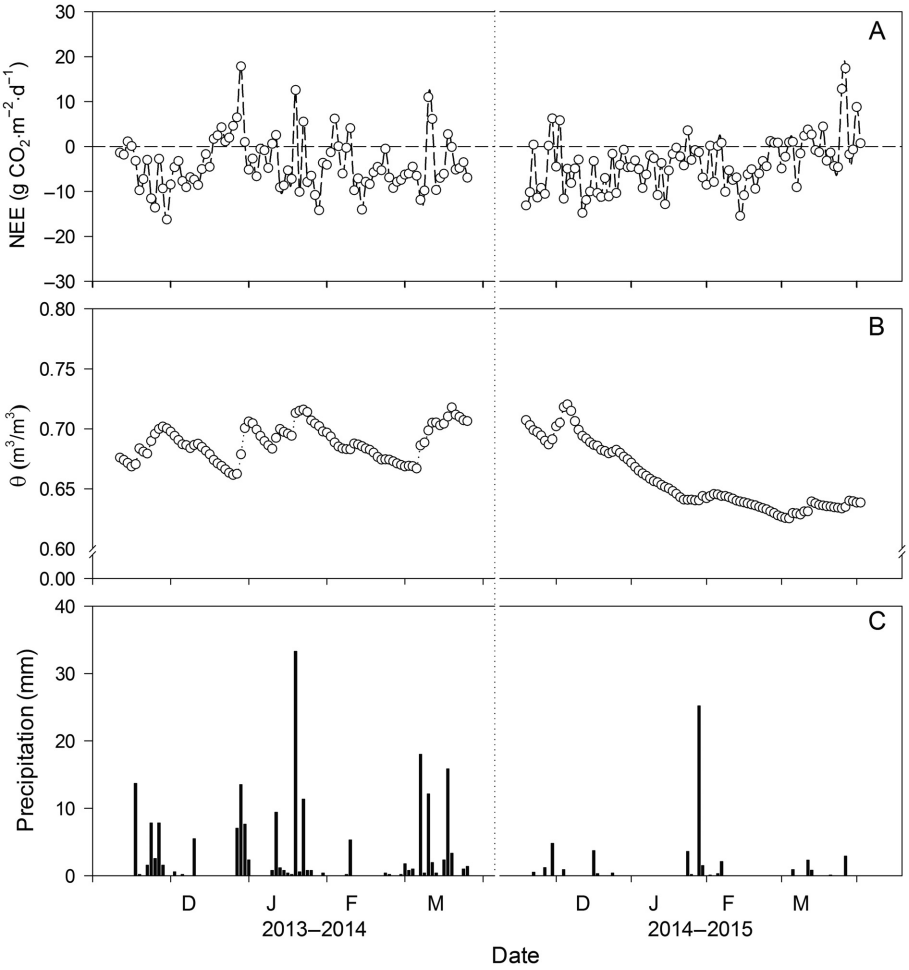

Fig. 6. Daily net ecosystem exchange (NEE; A), volumetric soil water content (θ; B), and precipitation (C) during two austral summer periods (January–March) for the two years of study discussed here, 2014 and 2015.

temperature of 14.4°C for both years, which is higher than the average estimated for the last 18 yr for this season (12.9°C) from meteorological records kept at the field station (Table 2). Summer precipitation was close to the 18-yr average in 2013–2014, but summer was exceedingly dry in 2014–2015, receiving only 128 mm of precipitation between December and March, which is less than half the average summer rainfall for the last 18 yr (Table 2). Fig. 6 compares the daily NEE of the two summer periods and the records for soil water content and precipitation. The data in Fig. 6 illustrate episodes when the forest switched from carbon sink to source (i.e., respiration exceeded carbon uptake by the ecosystem), which were more evident during the first year, even though the soil reached a drier condition in the second year (Fig. 6).

Comparison with other humid forest ecosystems

Over two years, the average annual carbon balance for this old-growth temperate rainforest represented a sink of -238 ± 31 g C/m^2, which is the result of a higher estimate of GPP (-2166 ± 150 g C/m^2) than R_{eco} (1914 ± 130 g C/m^2; Table 3). The net carbon uptake measured in the North Patagonian rainforest studied was lower than estimates for most temperate forests in the Northern Hemisphere and even lower than data for tropical evergreen, wet forests (Table 3). However, the values of GPP and R_{eco} of this forest are higher than for other northern temperate

Table 3. Climatic variables and carbon flux components (mean ± SD; g $C \cdot m^{-2} \cdot yr^{-1}$) in the SSA old-growth temperate evergreen broad-leaved rainforest recently added to global monitoring compared with other humid forest ecosystems from around the world.

Forest type†	No. sites	Micrometeorological variables						Fluxes‡		
		T	PP	T_{win}	T_{sum}	PP_{win}	PP_{sum}	GPP	R_{eco}	NEP
TE BL	1	9.7 ± 2.8	2087 ± 329	8 ± 2	14 ± 2	841 ± 163	288 ± 133	−2166 ± 150	1914 ± 130	−238 ± 31
TE NL	70	9.6 ± 4.4	1259 ± 577	4 ± 5	17 ± 4	449 ± 337	194 ± 234	−1762 ± 56	1336 ± 57	−398 ± 42
TD	67	10.5 ± 6.4	1009 ± 375	2 ± 9	20 ± 5	183 ± 164	356 ± 259	−1375 ± 56	1048 ± 64	−311 ± 38
TrE	35	20.2 ± 5.1	2795 ± 964	23 ± 4	24 ± 3	685 ± 664	469 ± 395	−3551 ± 160	3061 ± 162	−403 ± 102

Notes: T (°C), mean annual temperature; PP (mm), mean annual precipitation; T_{win} (°C), mean winter temperature; T_{sum} (°C), mean summer temperature; PP_{win} (mm), total winter precipitation; PP_{sum} (mm), total summer precipitation; GPP, gross primary productivity; R_{eco}, ecosystem respiration; NEP, net ecosystem productivity; SSA, southern South American; TE BL, temperate evergreen broad-leaved; TE NL, temperate evergreen needle-leaved; TD, temperate deciduous; TrE, tropical evergreen.

† Data organized by forest type, as reported by Luyssaert et al. (2007), to compare with our study site.

‡ Negative fluxes indicate ecosystem carbon uptake. We consider NEP to be equivalent to NEE, as discussed by Luyssaert et al. (2007).

forests, in this case closely resembling the values measured in tropical forests (Table 3).

The mean annual air temperature of this forest site in SSA is very similar to that of other temperate forests (~10°C), although the difference in mean temperature between winter and summer is much lower (6°C) than in the case of temperate evergreen needle-leaved (13°C) or temperate deciduous forests (18°C; N = 67 and 70 sites, respectively; Table 3). Accordingly, stability of seasonal temperatures makes this site more similar to the situation of tropical forests, although, overall, the mean annual temperature is half the value of tropical forests (9.7°C vs. 20.2°C; Table 3).

In terms of annual precipitation, the long-term average (2087 mm) of our study site is slightly lower than that of tropical forests reported by Luyssaert et al. (2795 mm) and twice as much as the long-term mean of 137 other temperate, needle-leaved and deciduous forest sites where carbon fluxes are presently being monitored (Table 3). Most of precipitation in SSA forests is recorded in winter, similar to what occurs in temperate needle-leaved evergreen forests but in contrast to what is observed in temperate deciduous forests (Table 3).

In terms of ecosystem carbon balance, the mean NEE of this forest is lower than that of other evergreen temperate forests measured (predominantly deciduous and needle-leaved) and even lower compared to most tropical forests where carbon fluxes have been measured (Table 3). However, the level of biological activity described for this site by the high GPP and R_{eco} is higher compared to northern temperate forests in the carbon flux database, which together with the reduced variability in temperature across seasons and the higher annual precipitation make the SSA temperate forest studied similar to a broad sample of tropical evergreen forests represented in the database (Table 3). Similarity in carbon-related ecosystem parameters is expected to be stronger if this SSA forest is compared specifically with tropical montane cloud forests, which, according to a review of 28 sites by Gotsch et al. (2016), have low temperature variability (14° ± 0.53°C), though higher than in the oceanic climate of SSA, with higher annual precipitation (3343 ± 282 mm).

Discussion

Until recently, old-growth forests worldwide were considered to be non-significant carbon sinks, as net biomass gain and primary productivity were nearly stalled in some old-growth compared to young, early successional stands (Chen et al. 2004). However, old-growth forests have been found to be even larger sinks (Tan et al. 2011), probably because for most species, biomass continues to increase with tree size, which means that old trees actively fix large amounts of carbon compared to smaller trees (Stephenson et al. 2014). Our results for this old-growth North Patagonian evergreen forest add to the increasing evidence that old-growth forests from tropical, boreal, and temperate regions

can be significant carbon sinks (Zhou et al. 2006, Luyssaert et al. 2008, Tan et al. 2011), and will continue to be so if global climate patterns remain similar. However, we also show that a broad-leaved, evergreen, temperate old-growth forest from SSA has higher biological activity during the year than its Northern Hemisphere counterparts because of the higher precipitation and the more stable temperature conditions across seasons, with largely snow-free winters. Because of the close-to-neutral carbon balance, the magnitude of the sink in our study site can be strongly dependent on the variability of climatic conditions, both seasonally and in response to climate change.

Even though the trend for NEE during both spring–summer periods in this old-growth SSA forest suggests a carbon sink at the ecosystem level (Table 2), the variable intensity of the summer drought characteristic of the site could make this forest ecosystem shift from carbon sink to source in some years (Fig. 6). Based on these considerations, slight increases in spring and especially summer temperatures along with marked reductions in precipitation during summer, as predicted by global and regional climate-change scenarios (IPCC 2013), can significantly impact the carbon sink capacity of this and other SSA forests. This implies that future reductions in summer precipitation due to climate change at southern temperate latitudes could deviate the regional system state from the condition of carbon sink, a change that has been already observed in old-growth, temperate needle-leaved forests (Falk et al. 2008, Wharton et al. 2012).

Therefore, as drier summers could potentially alter soil processes affecting tree growth (Gutiérrez et al. 2014), our data also show that warmer winters could make the ecosystem become a stronger carbon sink (Table 2). In fact, the higher sink observed in the first year of study (-260 g C/m^2) compared to the second one (-216 g C/m^2) was more strongly related to the difference in carbon fluxes observed in the first winter than to what occurred in spring or summer (Table 2). During winter of the first year, GPP reached higher values compared to the second year for the same level of solar radiation (Fig. 3). This may be simply explained by higher air temperatures recorded during winter in the first year (average 9.8°C) than in the second year (average 8.4°C). Lower air temperatures in the second-year winter did not increase R_{eco} as much as during the first year (Table 2). In summary, in our study site GPP seems to be the driving force of NEE. This finding coincides with that of Malhi et al. (2017), who found that GPP was the primary determinant of variations in net primary productivity in tropical montane forests in the Peruvian Andes. In contrast, our result differs from those of Falk et al. (2008), where R_{eco} was the most important driver of NEE for an evergreen needle-leaved forest in southern Washington State (USA).

While the summer of the second year (2014–2015) was much drier in this forest site compared to records from the previous 18 yr, it did not result in a smaller carbon sink (Table 2). A possible explanation for this result is that carbon sink behavior is due to differences in spring precipitation between years. Accordingly, precipitation in spring 2014–2015 was higher than in 2013–2014 (Table 2), which could mean that trees subjected to wetter spring had a stronger environmental buffer to tolerate the longer summer dry period of the second year. We believe that the relatively stable climatic conditions, documented by the lower seasonal variation in temperature between summer and winter in this SSA forest, compared to most Northern Hemisphere temperate forests (Table 3), could make the southern temperate ecosystem strongly sensitive to small changes in temperature and precipitation.

The consequences of repeated summer or spring droughts for tree growth and survival in North Patagonian forests are not well studied using long-term plots, but if such conditions become more frequent in the future, they could significantly alter ecosystem carbon dynamics. In this context, long-term measurements of carbon exchange at the ecosystem level in permanent study sites, such as our study site, in addition to the use of process-based models, will be essential to fully understand the mechanisms of carbon storage and loss and, therefore, our capacity to predict and mitigate climate-change impacts on the global carbon cycle. Presently, out of the 502 sites in the FLUXNET database representing natural ecosystems across the globe where carbon fluxes are being monitored, only 54 are in the

Southern Hemisphere (Fig. 7); as a consequence, we may be getting a biased picture of biosphere responses to global changes (FLUXNET 2016).

Most dynamic vegetation models that predict carbon storage capacity at a landscape scale have been based on data from a limited sample of evergreen, broad-leaved temperate forests. This low sample size results in elevated variability for this forest type, thus producing less robust carbon flux estimates (Luyssaert et al. 2007). Ground-based carbon budgets are lacking for forests in SSA, which are characterized by high soil carbon accumulation, and therefore, future assessments can greatly benefit from additional field data. For example, patterns in GPP and NEE in the global database (Luyssaert et al. 2007) show clear relationships with mean annual temperature and annual precipitation; however, for wet temperate forests receiving above 1500 mm of precipitation and having low seasonal variation in temperature, productivity may not follow this trend. Our site shows high biological activity (high GPP and R_{eco}) but lower carbon balance (net ecosystem productivity) compared to northern temperate forests (Table 3). We believe this could be explained mainly by the higher precipitation observed in our site, which is almost twice the average of both deciduous and needle-leaved temperate forests in the Northern Hemisphere, along with more stable temperature conditions of SSA forests (Table 3). Understanding the mechanisms explaining the uncoupling of biological activity patterns (inferred from the patterns of GPP and R_{eco}) and net carbon balance is part of an ongoing project that will use process-based modeling.

This new site (CL-SDF) in the global database of carbon flux monitoring (FLUXNET 2016) is the only active one measuring carbon exchanges in a SSA broad-leaved evergreen, temperate rainforest. According to this database, the only other active site located in a temperate forest in the Southern Hemisphere corresponds to a *Eucalyptus* forest in Australia (Code: AU-WOM). Broad-leaved, evergreen temperate rainforests of western SSA represent about one-half of the remaining distribution of this biome in the Southern Hemisphere and are the geographical and climatic

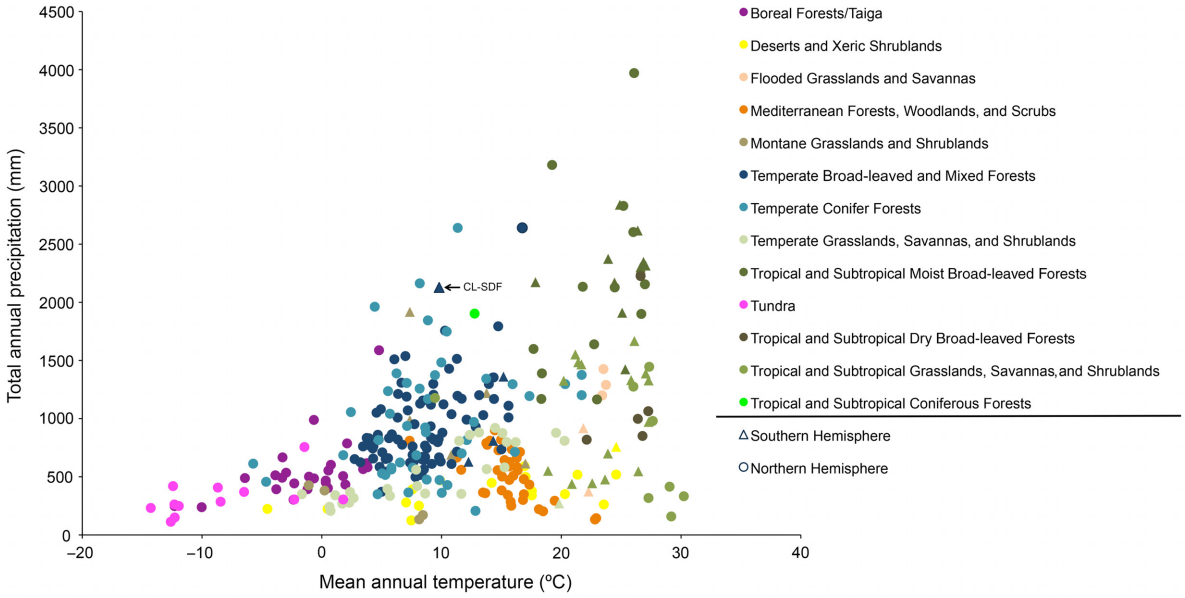

Fig. 7. Geographic distribution of the 502 FLUXNET sites monitoring carbon exchange in the global database for different biomes. Different color dots represent terrestrial ecoregions based on TNC classification (source: http://maps.tnc.org/gis_data.html). Circles and triangles represent sites in the Northern and Southern Hemisphere, respectively. The arrow indicates the new southern South American temperate rainforest site presented in this study (FLUXNET ID = CL-SDF), which was identified with the temperate broad-leaved and mixed forest biome (FLUXNET 2016).

counterparts of more extensive conifer-dominated rainforests in the Pacific Northwest of North America (Mooney et al. 1993, Lawford et al. 1996). Although limited in extent relative to their Northern Hemisphere counterparts, temperate rainforests in SSA store large volumes of biomass in live trees (Perez-Quezada et al. 2015) and slowly decomposing woody debris (Carmona et al. 2002), along with large amounts of organic carbon stored underground (Carmona et al. 2002, Armesto et al. 2009).

Because deforestation, degradation, and land use change can have direct implications for carbon sequestration and atmospheric carbon dynamics (Perez-Quezada et al. 2010, Pütz et al. 2014), the present study is designed to gather reliable information on present trends of carbon release and storage in a SSA old-growth rainforest ecosystem. A second monitoring site, located on a nearby anthropogenic peatland, in the same study area, where carbon stocks have been measured to show the effects of management (Cabezas et al. 2015) and an eddy covariance system is deployed (code CL-SDP), will make it possible to estimate the effect of deforestation on carbon fluxes, given that these peatlands emerge when forests over thin soils are clear-cut or burned. Data from the SSA sites should help model future trends of carbon dynamics in the face of impending climate change and other anthropogenic impacts, such as advancing deforestation and expanding forestry plantations (Echeverria et al. 2008, Gutiérrez et al. 2014, Heilmayr et al. 2016, Miranda et al. 2016).

Concluding Remarks

Based on carbon fluxes measured in this North Patagonian old-growth rainforest in SSA, we have gathered strong evidence for the relevance of this site to the global carbon cycle, which can be summarized as follows:

1. The seasonality of the forest ecosystem is low compared to typical Northern Hemisphere mid- or high-latitude forests considered as counterparts. Because of this climatic stability across seasons, this SSA forest shows events of carbon uptake during winter, when the ecosystem is primarily a carbon source, and episodes of carbon loss in summer, when the ecosystem is primarily a carbon sink.
2. The annual carbon balance remained negative over the study period. However, a weak seasonality can alter this condition, where NEE can switch to positive or negative depending on small changes in temperature or rainfall. We showed that summer drought can make the system switch from carbon sink to source, suggesting that precipitation is the main NEE driver during this season. During the winter, however, temperature seems to be an even stronger driver of NEE, making the system a sink when temperatures are above average.
3. Our results suggest that the functional response of this evergreen, North Patagonian forest ecosystem to global environmental changes resembles that of montane tropical forests, which are among the most endangered forest ecosystems worldwide. However, knowledge of the carbon dynamics of these tropical ecosystems is still rudimentary. Carbon dynamics and patterns measured in narrow-leaved, conifer-dominated evergreen temperate forests dominant over much of the Northern Hemisphere may not be applicable to other evergreen forests in the Southern Hemisphere or in tropical mountains.
4. Long-term monitoring of carbon exchanges in this temperate rainforest from SSA will offer new information for understanding the ecosystem mechanisms and environmental thresholds that could make an evergreen old-growth forest switch between carbon sink and source.

Acknowledgments

This work was supported by FONDEQUIP AIC-37, Iniciativa Científica Milenio grant P05-002 and CONICYT grant PFB-23 to the Institute of Ecology and Biodiversity-Chile (IEB), FONDECYT grant 1130935 to JPQ, and the LINCGlobal research program funded by CSIC-Spain and Catholic University of Chile. The authors thank Robert Cook and Alison Boyer, who kindly provided the FLUXNET database 2015. The

authors are grateful to Paul Reich (USDA) for sharing the Biome database, Sebastiaan Luyssaert for providing them with the database of CO_2 balance of forest ecosystems, and an anonymous reviewer whose comments helped them to improve the manuscript. This is a contribution to the Research Program of Senda Darwin Biological Station and the Chilean Long-Term Socio-Ecological Research Network (LTSER-Chile), affiliated with ILTER, AMERIFLUX, and FLUXNET.

Literature Cited

Aravena, J. C., M. R. Carmona, C. A. Pérez, and J. J. Armesto. 2002. Changes in tree species richness, stand structure and soil properties in a successional chronosequence in northern Chiloé Island, Chile. Revista Chilena de Historia Natural 75:339–360.

Armesto, J. J., C. Smith-Ramírez, M. R. Carmona, J. L. Celis-Diez, I. A. Díaz, A. Gaxiola, A. G. Gutiérrez, M. C. Núñez-Avila, C. A. Pérez, and R. Rozzi. 2009. Old-growth temperate rainforests of South America: conservation, plant–animal interactions, and baseline biogeochemical processes. Pages 367–385 *in* C. Wirth, G. Gleixner, and M. Heimann, editors. Old-growth forests. Ecological studies (analysis and synthesis). Volume 207. Springer, Berlin, Heidelberg, Germany.

Baldocchi, D. 2008. "Breathing" of the terrestrial biosphere: lessons learned from a global network of carbon dioxide flux measurement systems. Australian Journal of Botany 56:1–26.

Baldocchi, D. 2014. Measuring fluxes of trace gases and energy between ecosystems and the atmosphere: the state and future of the eddy covariance method. Global Change Biology 20:3600–3609.

Cabezas, J., M. Galleguillos, A. Valdés, J. P. Fuentes, C. Pérez, and J. F. Perez-Quezada. 2015. Evaluation of impacts of management in an anthropogenic peatland using field and remote sensing data. Ecosphere 6:282.

Carmona, M. R., J. Armesto, J. C. Aravena, and C. A. Perez. 2002. Coarse woody debris biomass in successional and primary temperate forests in Chiloé Island, Chile. Forest Ecology and Management 164:265–275.

Carmona, M. R., et al. 2010. Estación Biológica Senda Darwin: Investigación ecológica de largo plazo en la interfase ciencia-sociedad. Revista Chilena de Historia Natural 83:113–142.

Chen, J., K. T. Paw U, S. L. Ustin, T. H. Suchanek, B. J. Bond, K. D. Brosofske, and M. Falk. 2004. Net ecosystem exchanges of carbon, water, and energy in young and old-growth Douglas-fir forests. Ecosystems 7:534–544.

Coleman, T. F., and Y. Li. 1994. On the convergence of interior-reflective Newton methods for nonlinear minimization subject to bounds. Mathematical Programming 67:189–224.

Di Castri, F., and E. Hajek. 1976. Bioclimatología de Chile. Universidad Católica de Chile, Santiago, Chile.

Echeverria, C., D. A. Coomes, M. Hall, and A. C. Newton. 2008. Spatially explicit models to analyze forest loss and fragmentation between 1976 and 2020 in southern Chile. Ecological Modelling 212: 439–449.

Falge, E., et al. 2001. Gap filling strategies for defensible annual sums of net ecosystem exchange. Agricultural and Forest Meteorology 107:43–69.

Falk, M., S. Wharton, M. Schroeder, S. L. Ustin, and K. T. Paw U. 2008. Flux partitioning in an old-growth forest: seasonal and interannual dynamics. Tree Physiology 28:509–520.

FLUXNET. 2016. A global network. https://fluxnet.ornl.gov

Friend, A. D., A. Arneth, N. Y. Kiang, M. Lomas, J. Ogee, C. Rödenbeck, S. W. Running, J.-D. Santaren, S. Sitch, and I. F. Woodward. 2007. FLUXNET and modelling the global carbon cycle. Global Change Biology 13:610–633.

Gotsch, S. G., H. Asbjornsen, and G. R. Goldsmith. 2016. Plant carbon and water fluxes in tropical montane cloud forests. Journal of Tropical Ecology 32:404–420.

Gutiérrez, A. G., J. J. Armesto, and J. C. Aravena. 2004. Disturbance and regeneration dynamics of an old-growth North Patagonian rain forest in Chiloé Island, Chile. Journal of Ecology 92:598–608.

Gutiérrez, A. G., J. J. Armesto, M. F. Díaz, and A. Huth. 2014. Increased drought impacts on temperate rainforests from Southern South America: results of a process-based, dynamic forest model. PLoS ONE 9:37–43.

Hedin, L. O., J. J. Armesto, and A. H. Johnson. 1995. Patterns of nutrient loss from unpolluted old growth temperate forests: evaluation of biogeochemical theory. Ecology 76:493–509.

Heilmayr, R., C. Echeverría, R. Fuentes, and E. F. Lambin. 2016. A plantation-dominated forest transition in Chile. Applied Geography 75:71–82.

IPCC. 2013. Annex I: Atlas of global and regional climate projections. *In* G. J. van Oldenborgh, M. Collins, J. Arblaster, J. H. Christensen, J. Marotzke, S. B. Power, M. Rummukainen, and T. Zhou, editors. Climate change 2013: the physical science basis. Contribution of Working Group I to the Fifth Assessment Report of the Intergovernmental Panel on Climate Change [T. F. Stocker, D. Qin,

G.-K. Plattner, M. Tignor, S. K. Allen, J. Boschung, A. Nauels, Y. Xia, V. Bex, and P. M. Midgley, editors]. Cambridge University Press, Cambridge, UK and New York, New York, USA.

Kljun, N., P. Calanca, M. W. Rotach, and H. P. Schmid. 2004. A simple parameterisation for flux footprint predictions. Boundary-Layer Meteorology 112:503–523.

Lasslop, G., M. Reichstein, D. Papale, A. Richardson, A. Arneth, A. Barr, P. Stoy, and G. Wohlfahrt. 2010. Separation of net ecosystem exchange into assimilation and respiration using a light response curve approach: critical issues and global evaluation. Global Change Biology 16:187–208.

Lawford, R., P. Alaback, and E. Fuentes. 1996. High-latitude rainforests and associated ecosystems of the west coast of the Americas: climate, hydrology, ecology, and conservation. Springer-Verlag, New York, New York, USA.

Leys, C., C. Ley, O. Klein, P. Bernard, and L. Licata. 2013. Detecting outliers: Do not use standard deviation around the mean, use absolute deviation around the median. Journal of Experimental Social Psychology 49:764–766.

Luyssaert, S., E.-D. Schulze, A. Börner, A. Knohl, D. Hessenmöller, B. E. Law, P. Ciais, and J. Grace. 2008. Old-growth forests as global carbon sinks. Nature 455:213–215.

Luyssaert, S., et al. 2007. CO_2 balance of boreal, temperate, and tropical forests derived from a global database. Global Change Biology 13:2509–2537.

Malhi, Y., et al. 2017. The variation of productivity and its allocation along a tropical elevation gradient: a whole carbon budget perspective. New Phytologist 214:1019–1032.

Mauder, M., and T. Foken. 2004. Documentation and instruction manual of the eddy covariance software package TK2. Abt. Mikrometeorologie, Universität Bayreuth, Bayreuth, Germany.

Miranda, A., A. Altamirano, L. Cayuela, A. Lara, and M. González. 2016. Native forest loss in the Chilean biodiversity hotspot: revealing the evidence. Regional Environmental Change 17:285–297.

Mittermeier, R. A., C. G. Mittermeier, T. M. Brooks, J. D. Pilgrim, W. R. Konstant, G. A. da Fonseca, and C. Kormos. 2003. Wilderness and biodiversity conservation. Proceedings of the National Academy of Sciences USA 100:10309–10313.

Moffat, A. M., et al. 2007. Comprehensive comparison of gap-filling techniques for eddy covariance net carbon fluxes. Agricultural and Forest Meteorology 147:209–232.

Mooney, H., E. R. Fuentes, and B. I. Kronberg. 1993. Earth system responses to global change. Contrasts between North and South America. Academic Press, New York, New York, USA.

Muñoz, A., P. Chacon, F. Perez, E. S. Barnert, and J. J. Armesto. 2003. Diversity and host tree preferences of vascular epiphytes and vines in a temperate rainforest in southern Chile. Australian Journal of Botany 51:381–391.

Perez-Quezada, J. F., S. Olguín, J. P. Fuentes, and M. Galleguillos. 2015. Tree carbon stock in evergreen forests of Chiloé, Chile. Bosque 36:27–39.

Perez-Quezada, J. F., N. Z. Saliendra, K. Akshalov, D. A. Johnson, and E. A. Laca. 2010. Land use influences carbon fluxes in northern Kazakhstan. Rangeland Ecology and Management 63:82–93.

Pütz, S., J. Groeneveld, K. Henle, C. Knogge, A. C. Martensen, M. Metz, J. P. Metzger, M. C. Ribeiro, M. D. de Paula, and A. Huth. 2014. Long-term carbon loss in fragmented Neotropical forests. Nature Communications 5:5037.

Reichstein, M., et al. 2005. On the separation of net ecosystem exchange into assimilation and ecosystem respiration: review and improved algorithm. Global Change Biology 11:1424–1439.

Rozzi, R., et al. 2012. Integrating ecology and environmental ethics: earth stewardship in the southern end of the Americas. BioScience 62:226–236.

Stephenson, N. L., et al. 2014. Rate of tree carbon accumulation increases continuously with tree size. Nature 507:90–93.

Tan, Z. H., Y. P. Zhang, D. Schaefer, G. R. Yu, N. Liang, and Q. H. Song. 2011. An old-growth subtropical Asian evergreen forest as a large carbon sink. Atmospheric Environment 45:1548–1554.

Weathers, K., G. Lovett, G. Likens, and N. F. M. Caraco. 2000. Cloudwater inputs of nitrogen to forest ecosystems in southern Chile: forms, fluxes, and sources. Ecosystems 3:590–595.

Wharton, S., M. Falk, K. Bible, and M. Schroeder. 2012. Old-growth CO_2 flux measurements reveal high sensitivity to climate anomalies across seasonal, annual and decadal time scales. Agricultural and Forest Meteorology 161:1–14.

Zhou, G., S. Liu, Z. Li, D. Zhang, X. Tang, C. Zhou, J. Yan, and J. Mo. 2006. Old-growth forests can accumulate carbon in soils. Science 314:1417.

Supporting Information

Additional Supporting Information may be found online at: http://onlinelibrary.wiley.com/doi/10.1002/ecs2.2193/full